BENZIMIDAZOLE-DERIVED METAL COMPLEXES: STRUCTURAL INSIGHTS AND ANTIMICROBIAL POTENTIAL AGAINST *STAPHYLOCOCCUS AUREUS* AND *ESCHERICHIA COLI*

S.M. AL-Asalli, F.T. Saeed, H.Y. Hussien

Department of Chemistry, College of Science, University of Mosul, Mosul, Iraq.
e-mail: farah-t-s@uomosul.edu.iq

Received 13.08.2025
Accepted 21.10.2025

Abstract: *The stable metal complexes of transition metals with benzimidazole derivatives lead to improved physicochemical and biological properties of these compounds. The development of antimicrobial agents becomes possible through complex design based on benzimidazole-derived compounds. The research focused on creating and analyzing bis((1H-benzo[d]imidazol-2-yl)methyl)sulfane (L) as a benzimidazole-derived ligand and studying its Mn(II), Co(II), Ni(II), Cu(II), and Zn(II) metal complexes. The researchers synthesized the ligand and its metal complexes through sequential steps before using elemental analysis and FTIR and UV–Vis and ^{1}H-NMR and conductivity and magnetic measurements for identification. The agar well diffusion method served to evaluate the antibacterial properties of the compounds against Staphylococcus aureus and Escherichia coli.*

The spectroscopic and analytical results showed that the imidazole nitrogen atoms of the ligand act as binding sites, while the thioether sulfur atom does not participate in coordination. The complexes showed tetrahedral structures that existed as $[M(L)_2]Cl_2$ or $[M_2(L)_2(H_2O)_2]Cl_2$ compounds. The results from antibacterial tests revealed that metal complexation led to substantial improvements in biological activity. The Cu(II) complexes produced the largest inhibition zones, while the Zn(II) complexes showed the second-highest activity, and both complexes displayed better effects against S. aureus than E. coli.

Benzimidazole-based ligands serve as effective building blocks for creating transition metal complexes, which show promising antimicrobial activity according to the research findings. The improved activity of Cu(II) and Zn(II) complexes indicates that chelation enhances both lipophilicity and bacterial membrane permeability.

Keywords: *Benzimidazole ligand; Transition metal complexes; Spectroscopic characterization; Tetrahedral geometry; Chelation theory; Antibacterial activity; Staphylococcus aureus; Escherichia coli*

Introduction

The bicyclic structure of benzimidazole derivatives makes them privileged heteroaromatic systems because it combines stability with biological versatility through their fused benzene and imidazole ring system [1]. The medicinal and bioinorganic field values benzimidazole scaffolds because their benzene–imidazole structure enables dual hard/soft donor sites and adjustable lipophilicity and chemical stability, which work together to achieve specific metal binding and biological target interaction (Fig. 1). The exploration of benzimidazole-containing compounds continues in antimicrobial, antifungal, antiviral, and anticancer research because metal coordination with first-row transition metals enhances drug penetration and controls redox reactions and strengthens DNA/protein interactions through increased apparent lipophilicity. The structural elements of benzimidazole-based ligands enable their application in catalysis and chemical sensing, which demonstrates their wide-ranging potential through direct relationships between molecular features and biological and solution-based performance [2, 3].

The conceptual framework enables researchers to understand benzimidazole complex structure–activity relationships (SAR) through three connected factors, which include metal identity/geometry effects on d–d transitions and redox potential and coordination dynamics; ligand topology and donor preference effects on metal center electronic distribution and sterics; and solution behavior and speciation effects on solubility and ion pairing and bioavailability.

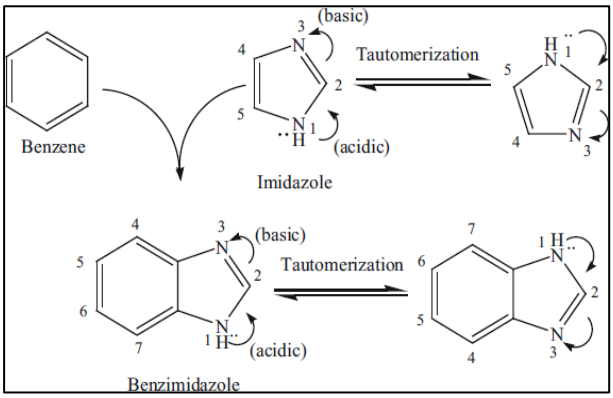

Fig. 1. Structural representation of the fused benzene–imidazole system and the tautomeric interconversion between imidazole and benzimidazole

The redox properties of Cu(II) and Zn(II) centers make them more effective than free ligands at fighting Gram-positive bacteria because these centers can easily penetrate the bacterial envelope structure. The study functions as a mechanistic investigation that examines how tetrahedral coordination structures and imidazole-N binding affect antimicrobial activity. Benzimidazole derivatives function as pharmacophores in established drugs, including albendazole, omeprazole, and mebendazole, which show anthelmintic and proton-pump inhibitory effects through binding to enzymatic and membrane-associated targets. The benzimidazole framework shows how changes at the 2-position and N-functionalization lead to significant effects on target binding properties and metabolic stability. The combination of this heterocyclic structure with transition metal coordination produces new compounds that unite synthetic coordination chemistry with medicinal applications through their dual benefits of physical and biological properties.

The imidazole ring structure in these compounds enables them to duplicate the natural behavior of purines, which results in their involvement in fatty acid biosynthesis and purine nucleotide production [3]. The biomedical significance and therapeutic value of benzimidazole units become stronger because they form part of vitamin B12's structure [4, 5].

Benzimidazole-based ligands serve as effective chelating agents in coordination chemistry because their imidazole ring nitrogen atoms enable efficient binding to transition metals, including Mn(II), Co(II), Ni(II), Cu(II), and Zn(II) [6, 7]. Schiff bases made from benzimidazole show broad biological applications, including antimicrobial, antifungal, and anticancer effects, which stem from their coordination properties [8, 9]. The complexes show multiple applications in catalysis and corrosion inhibition and the polymer and dye industries because of their diverse functional properties [10, 11]. Benzimidazole derivatives attract increasing pharmaceutical interest because their molecular structure matches nucleic acid bases and their ability to create stable metal ion complexes [12, 13]. Research shows that 2-substituted benzimidazole compounds with antiviral and antitumor effects support the role of metal coordination in biological activity regulation [14, 15].

This research aimed to develop a new ligand via transformation of a benzimidazole precursor into bis((1H-benzo[d]imidazol-2-yl)methyl)sulfane and to investigate its coordination behavior with Mn(II), Co(II), Ni(II), Cu(II), and Zn(II) salts. The synthesized metal complexes were characterized by elemental analysis, FT-IR, UV–Vis spectroscopy, ^{1}H-NMR spectroscopy, and molar conductivity measurements to elucidate their structural features. In addition, the antibacterial activity of the ligand and its metal complexes was evaluated against *Staphylococcus aureus* (Gram-positive) and *Escherichia coli* (Gram-negative) to assess the influence of metal coordination on biological activity [16, 17].

Experimental part

Chemicals and Reagents. The study used entirely chemicals and solvents that were of analytic grade and obtained from commercial suppliers BDH and Fluka. The researchers checked the purity of all reagents before starting work and skipped any additional purification steps.

The researchers used all reagents at analytical grade (≥99% purity) without further treatment. The benzimidazole precursors needed desiccators for storage at room temperature to stop moisture absorption. The researchers used thin-layer chromatography to check for byproducts during chloroacetic acid amidation and substitution reactions because they wanted to confirm that the chlorine atom did not disrupt amide bond formation when the reaction occurred under reflux conditions.

Instrumentation. The researchers used spectroscopic and analytical methods to study the structural and elemental properties of the ligand together with its metal complexes.

The FT-IR spectra were recorded between 4000 and 400 cm^{-1} using KBr pellets on a Bruker Tensor 27co spectrophotometer [24].

The LCHN-ALO analyzer (UK) performed elemental analysis of C, H, and N elements through standard microanalytical procedures [24].

The AA670 atomic absorption spectrophotometer determined the metal content of the samples.

The Shimadzu UV–Vis 160 spectrophotometer recorded electronic spectra of solutions containing 10^{-3} M DMSO at 25 °C [18].

The PCM3 Jenway conductivity meter measured molar conductivity of DMSO solutions at room temperature to determine their electrolytic properties [19].

The ^{1}H-NMR spectroscopy results verified both the ligand structure and the substitution patterns of the compounds.

Synthesis of the Ligand. Ligand bis((1H-benzo[d]imidazol-2-yl)methyl)sulfane (L) was prepared through a sequence of chemical reactions involving an acceptor–donor mechanism, in which the deprotonated imidazole nitrogen atom attacks an electrophilic center. The synthesis proceeds via nucleophilic substitution at a donor carbon atom, leading to the formation of a thioether bond. The mechanism of this process appears in Figure 2, which demonstrates how the Cu(II) complex binds to imidazole-N donors.

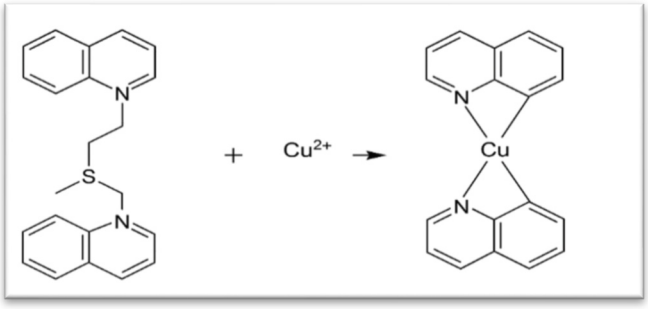

Fig. 2. Proposed donor–acceptor mechanism for Cu(II) complex formation

1. ***Preparation of precursor (A)****:* 2-(chloromethyl)-1H-benzimidazole was obtained by reacting chloroacetic acid with *o*-phenylenediamine in hydrochloric acid under reflux for 6 h. The progress of the reaction was managed by thin-layer chromatography (TLC) using ethyl acetate: petroleum ether as the mobile phase. The yellow precipitate was neutralized with concentrated NH_3, filtered, and recrystallized from methanol (m.p. 147 °C) [20].

2. ***Preparation of precursor (B)****:* 2-(mercaptomethyl)-1H-benzimidazole was synthesized by a similar route, replacing chloroacetic acid with thioglycolic acid. The reaction afforded a pale-yellow product (m.p. 158 °C) [21].

3. ***Formation of ligand (L)****:* Precursor (A) (1.64 g, 0.01 mol) was first dissolved in alkaline methanol prepared from 0.56 g of KOH in 40 mL of methanol and magnetically stirred for 30 minutes. To this solution, precursor (B) (1.66 g, 0.01 mol), previously dissolved in methanol, was introduced, and the mixture was refluxed for 3 hours. The reaction afforded a white solid, which was collected by filtration, thoroughly washed, and recrystallized from methanol to give a product with a melting point of 221 °C [22].

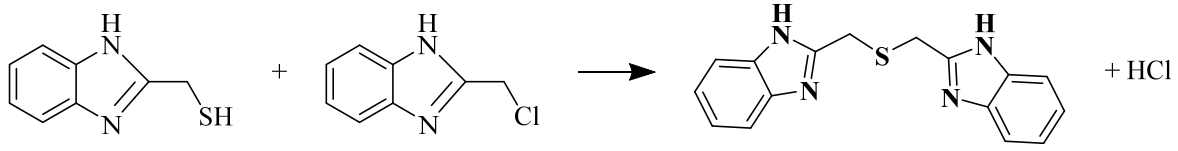

Synthesis of Metal Complexes. The ligand (L) was allowed to react with chloride salts of Mn(II), Co(II), Ni(II), Cu(II), and Zn(II) (Table 1), affording complexes of the general formulas $[M(L)_2]Cl_2$ and $[M_2(L)_2(H_2O)_2]Cl_2$.

- **$[M(L)_2]Cl_2$ complexes:** A methanolic solution of the corresponding metal salt (0.001 mol in 10 mL) was gradually introduced into a hot methanolic solution of the ligand (0.002 mol in 10 mL). The mixture was refluxed under continuous stirring for 3 hours, giving rise to a solid product that was collected by filtration, rinsed sequentially with cold methanol and diethyl ether, and finally dried under vacuum.
- **$[M_2(L)_2(H_2O)_2]Cl_2$ complexes:** The same experimental procedure was applied, except that 0.002 mol of the metal salt was employed.

All complexes were obtained as stable solids, resistant to atmospheric moisture and suitable for subsequent analytical and biological studies.

Table 1. The weight (0.025 mol) metal salt

Metal salts	Weight gm (0.001 mol)	Weight gm (0.002 mol)
$MnCl_2.4H_2O$	0.24	0.48
$CoCl_2.6H_2O$	0.29	0.59
$NiCl_2.6H_2O$	0.28	0.59
$CuCl_2.2H_2O$	0.21	0.42
$ZnCl_2$	0.16	0.32

Antibacterial Activity. The antibacterial potential of the ligand together with its Cu(II) and Zn(II) complexes was evaluated against *Staphylococcus aureus* (Gram-positive) and *Escherichia coli* (Gram-negative) employing the agar well diffusion assay. Test solutions were prepared in dimethylformamide (DMF) at a concentration of 3 mg/mL. From each solution, 50 µL aliquots were dispensed into 6 mm wells previously made in nutrient agar plates seeded with bacterial suspensions standardized to 0.5 McFarland turbidity. The plates were then incubated at 37 °C for 24 hours, after which the diameters of the inhibition zones (mm) were recorded. DMF was used as the solvent control, and each test was carried out in triplicate [25–27].

Results and Discussion

Elemental and Physicochemical Properties. The spectroscopic and analytical evidence collectively delineates a clear structure–activity pattern across the synthesized complexes. Variations in ν(C=N) stretching frequencies, magnetic moments, and electronic transitions correlate strongly with the identity of the coordinating metal center. This structure–property–activity relationship (SAR) suggests that increasing crystal field stabilization and moderate ligand-field asymmetry, particularly in Cu(II) and Zn(II) complexes, enhances redox flexibility and favors membrane interaction, thereby elevating antimicrobial potency.

The ligand bis((1H-benzo[d]imidazol-2-yl)methyl)sulfane (L) existed in pure form because it showed a distinct melting point, and its elemental composition remained constant. The experimental C, H, and N percentage measurements of the ligand and its metal complexes matched the theoretical values, which validated the molecular structures and stoichiometric ratios. The majority of Cu(II) complexes reached high yields between 80-96% because they formed stable coordination compounds (Table 2). The elemental analysis results for the C, H, and N elements of both the ligand and complexes showed perfect agreement with theoretical values, which validated the proposed molecular structures [23].

The compounds showed dissolution in DMSO and DMF but failed to dissolve in hexane and chloroform due to their ionic properties. The compounds showed the expected ionic behavior through their solubility pattern, which enabled further spectroscopic and biological assessments.

Table 2. Physicochemical and analytical characteristics of the ligand and its metal complexes

No	Compound formula	Yield, %	Color	M.p., °C	Elemental Analysis Calculated (found)%			Molar conductivity, $Ohm^{-1}\cdot Cm^{-1}\cdot Mol^{-1}$
					C	H	N	
A	$C_8H_7N_2Cl$	77	Yellow	147-149	57.67 (57.35)	4.23 (4.21)	16.81 (16.65)	----
B	$C_8H_8N_2S$	88	Pale yellow	158-160	58.51 (58.22)	4.91 (4.66)	17.06 (16.81)	----
L	$C_{16}H_{14}N_4S$	82	White	230-232	65.28 (65.03)	4.79 (4.43)	19.03 (18.82)	----
1	$[Mn(L)_2]Cl_2$	95	Brown yellow	254-256	53.78 (53.67)	3.94 (3.75)	15.68 (15.44)	70
2	$[Co(L)_2]Cl_2$	85	Blue	300*	53.48 (53.22)	3.92 (3.74)	15.59 (15.23)	76
3	$[Ni(L)_2]Cl_2$	94	Dark green	255-257	53.50 (53.35)	3.92 (3.78)	15.59 (15.35)	73
4	$[Cu(L)_{2]}Cl_2$	85	Green	246-248	53.19 (52.97)	3.90 (3.79)	15.49 (15.22)	75
5	$[Zn(L)_{2]}Cl_2$	88	White	303-305	53.00 (52.88)	3.89 (3.53)	15.45 (15.33)	76
6	$[Mn_2(L)_2(H_2O)_2]Cl_4$	78	Off white	290-292	42.11 (41.86)	3.97 (3.51)	12.27 (11.45)	88
7	$[Co_2(L)_2(H_2O)_2]Cl_4$	88	Blue-green	297*	41.75 (41.33)	3.94 (3.52)	12.17 (11.59)	90
8	$[Ni_2(L)_2(H_2O)_2]Cl_4$	89	Green	300*	41.77 (41.35)	3.94 (3.49)	12.17 (11.81)	89
9	$[Cu_2(L)_2(H_2O)_2]Cl_4$	96	Dark green	210-212	4.134 (40.70)	3.90 (3.39)	12.05 11.71)	84
10	$[Zn_2(L)_2(H_2O)_2]Cl_4$	86	Off white	318-320	41.17 (40.33)	3.88 (3.43)	12.00 (11.81)	88

* = *decomposes*

The complexes formed stable solid compounds that showed no water absorption and maintained stability under normal environmental conditions. The pure products and reliable synthesis method became evident through their distinct melting points. The metal coordination resulted in lattice

stability enhancement because the complexes showed melting points that exceeded the free ligand value.

The DMSO solution tests showed that $[M(L)_2]Cl_2$ complexes function as electrolytes because they contain free chloride ions. The solution ionic dissociation of dinuclear $[M_2(L)_2(H_2O)_2]Cl_2$ complexes exceeded that of the mononuclear $[M(L)_2]Cl_2$ complexes according to their measured conductivity values [24]. The ionic nature of the complexes became evident through these results, which also validated the existence of both mono- and dinuclear species.

Infrared Spectral Analysis. The FTIR spectra provided further evidence for coordination (Table 3 and Fig. 3).

Table 3. Distinctive IR Spectral Features of the Ligands and their Metal Complexes

No.	Compound	ν (C=N)	ν (NH)	ν (C-S)	ν (C=C) aromatic	ν (M-N)	OH_2	Cl ionic
L	$C_{16}H_{14}N_4S$	1600	3172	733	1625	---	---	---
1	$[Mn(L)_2]Cl_2$	1580	3167	733	1623	437	-----	619
2	$[Co(L)_2]Cl_2$	1583	3170	734	1624	437	-----	619
3	$[Ni(L)_2]Cl_2$	1581	3172	733	1621	429	-----	619
4	$[Cu(L)_2]Cl_2$	1575	3173	734	1621	438	------	625
5	$[Zn(L)_2]Cl_2$	1579	3170	733	1624	469	------	620
6	$[Mn_2(L)_2(H_2O)_2]Cl_2$	1581	3170	734	1624	436	3443	619
7	$[Co_2(L)_2(H_2O)_2]Cl_2$	1620	3372	733	1626	484	3554	619
8	$[Ni_2(L)_2(H_2O)_2]Cl_2$	1580	3172	736	1621	421	3396	582
9	$[Cu_2(L)_2(H_2O)_2]Cl_2$	1582	3172	733	1623	429	3314	614
10	$[Zn_2(L)_2(H_2O)_2]Cl_2$	1580	3169	733	1622	472	3353	618

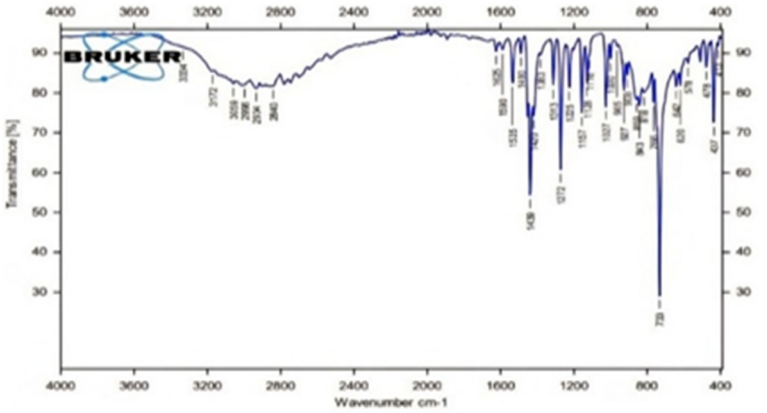

(a)

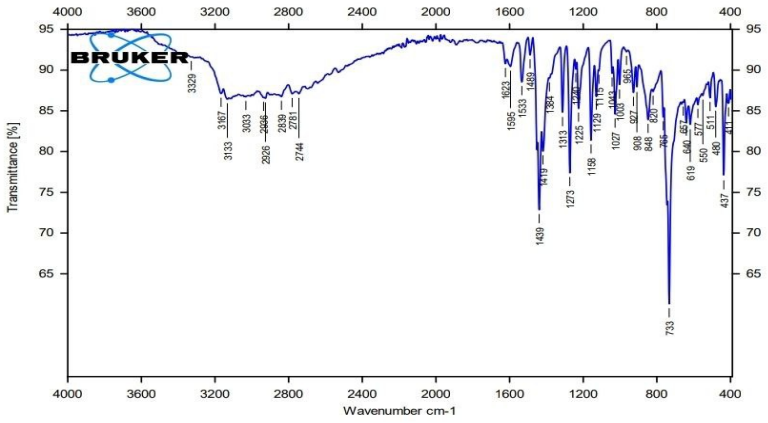

(b)

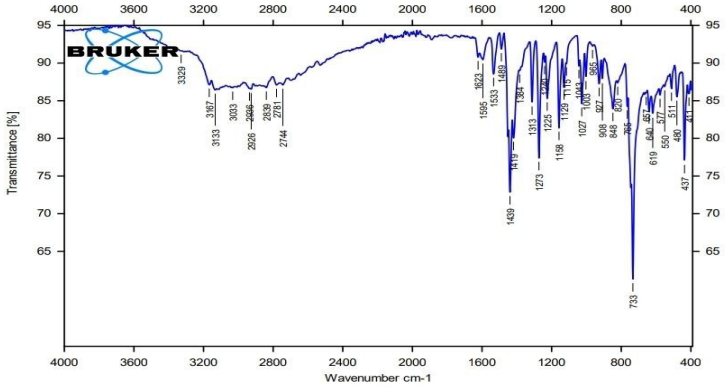

(c)

Fig. 3. The IR spectrum of (a)L,(b) $[Mn(L)_2]Cl_2$, (c) $[Ni_2(L)_2H_2O]Cl_2$

The FTIR spectrum of the free ligand shows the ν(C=N) stretching band at 1590 cm^{-1}, which confirms the imidazole structure. The metal coordination of the imidazole nitrogen atom becomes evident through the 1574–1620 cm^{-1} band shift, which occurs after complex formation [25]. The FTIR spectrum shows new bands between 421 and 421–484 cm^{-1}, which prove the formation of metal-nitrogen bonds [26]. The 3314–3545 cm^{-1} range contains broad signals that confirm the presence of water molecules that bind to the metal centers [27]. The thioether sulfur atom in the complex shows no change in its ν(C–S) band position at 733 cm^{-1}, which indicates it does not form bonds with the metal. The benzimidazole ligand coordination behavior matches previous research findings [28]. The imidazole NH stretching band of the ligand shifts slightly from 3245 to 3260; the imidazole NH participates in hydrogen bonding stabilization. However, no significant coordination through NH was detected, confirming that the primary donor sites were the ring nitrogen atoms. The thioether ν(C–S) band appeared around 733 cm^{-1} in the free ligand and remained unaltered in the spectra of all complexes, thereby confirming that the sulfur atom of the thioether moiety did not participate in coordination.

Electronic Spectra and Magnetic Moments. The ligand exhibited two characteristic bands at 42,134 and 44,325 cm^{-1}, allotted to π→π* and n→π* transitions. In contrast, the complexes exhibit additional d–d transitions consistent with tetrahedral geometries. For example, Co(II) complexes displayed absorptions near 14,321–14,423 cm^{-1}, typical of $^4A_2(F) \rightarrow {}^4T_1$ transitions. The corresponding μ_{eff} values (4.8–5.0 B.M.) also supported tetrahedral assignment (Table 4). Representative UV–Vis spectra are provided in Fig. 4 [29].

Table 4. Electron spectra and magnetic moments of ligands and its compounds

No.	Complex	Transition		μ_{eff}, (B.M.)
L	$C_{16}H_{14}N_4S$	421340 443251	π → π* n → π*	----
1	$[Mn(L)_2]Cl_2$	39675 38790 34310	π → π* n → π* C.T	6.1
2	$[Co(L)_2]Cl_2$	14321 39679	$^4A_2g(F) \rightarrow {}^4T_1(P)$ C.T	4.82
3	$[Ni(L)_2]Cl_2$	14567 31342 13890 35773	π → π* n → π* $^3T_1(F) \rightarrow {}^3T_1(p)$ C.T	2.58
4	$[Cu(L)_2]Cl_2$	13873 32786	$^2Eg \rightarrow {}^2T_1g$ C.T	1.80
5	$[Zn(L)_2]Cl_2$	36769	C.T	Dia
6	$[Mn_2(L)_2(H_2O)_2]Cl_2$	46523 39021	π π* ⟶ n π* ⟶	1.49

		34287	C.T	
7	$[Co_2(L)_2(H_2O)_2]Cl_2$	14423 32548	$^4A_2g(F) \rightarrow {}^4T_1(P)$ C.T	5.03
8	$[Ni_2(L)_2(H_2O)_2]Cl_2$	14398 32450 13801 36732	$\pi \rightarrow \pi^*$ $n \rightarrow \pi^*$ $^3T_1(F) \rightarrow {}^3T_1(p)$ C.T	2.79
9	$[Cu_2(L)_2(H_2O)_2]Cl_2$	14899 33256	$^2Eg \rightarrow {}^2T_1g$ C.T	2.63
10	$[Zn_2(L)_2(H_2O)_2]Cl_2$	32436	C.T	Dia

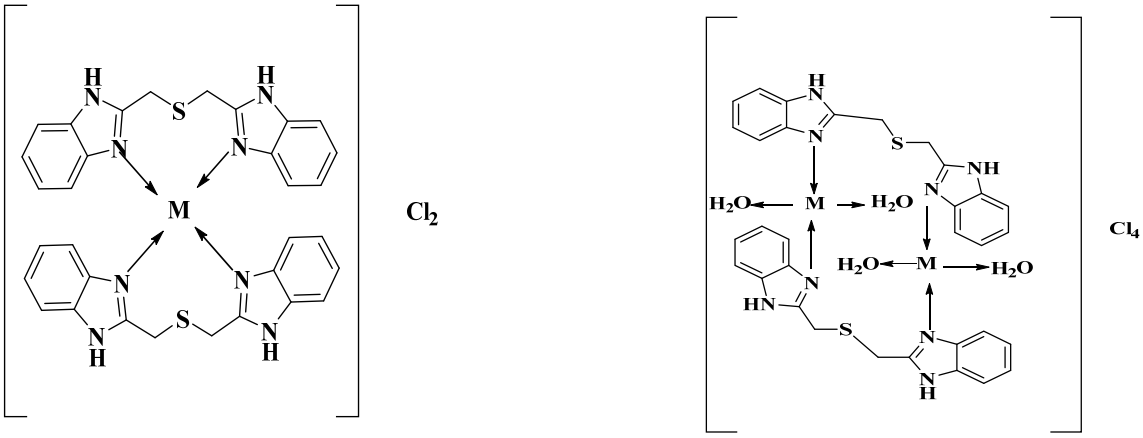

Fig. 4. Proposed geometrical structures of $M(L)_2]Cl_2$ (a) and $[M_2(L)_2(H_2O)_2]Cl_2$ (b) complexes

For Co(II) complexes, in addition to the 14,321–14,423 cm^{-1} band assigned to the $^4A_2(F) \rightarrow {}^4T_1(P)$ transition, a weaker absorption around 8,200–8,500 cm^{-1} was observed, corresponding to the $^4A_2(F) \rightarrow {}^4T_1(F)$ transition. This further substantiates the assignment of a distorted tetrahedral geometry. Similarly, Ni(II) complexes displayed bands at ~8,700 cm^{-1} and 14,400 cm^{-1}, attributed to $^3T_1(F) \rightarrow {}^3A_2(F)$ and $^3T_1(F) \rightarrow {}^3T_2(P)$ transitions, respectively. These absorptions, coupled with μ_eff values around 2.6–2.8 B.M., are characteristic of tetrahedral Ni(II) systems.

In the metal complexes, additional absorptions were observed:

- **Mn(II):** weak d–d transitions typical of high-spin tetrahedral Mn(II) with μ_eff values around 6.1 B.M., confirming a d^6 configuration [30].
- **Co(II):** bands at 14,321–14,423 cm^{-1} correspond to $^4A_2(F) \rightarrow {}^4T_1$ transitions in distorted tetrahedral geometry, supported by μ_eff values of 4.8–5.0 B.M. [38, 39].
- **Ni(II):** absorptions at ~14,400 cm^{-1} are characteristic of $^3T_1(F) \rightarrow {}^3T_1(P)$ transitions, consistent with tetrahedral Ni(II), with μ_eff ~2.6–2.8 B.M. [30].
- **Cu(II):** broad absorptions around 13,800–14,900 cm^{-1} reflect $^2T_2 \rightarrow {}^2E$ transitions, supported by μ_eff values of 1.8–2.6 B.M., indicating a single unpaired electron [31].
- **Zn(II):** no d–d transitions were observed, but charge-transfer bands at 32,436–36,769 cm^{-1} were evident, as expected for diamagnetic d^{10} systems [28].

These results confirm tetrahedral geometries for all complexes, supported by both spectral and magnetic data.

Stability and Solubility. The complexes were stable under dry air and soluble in common organic solvents, enabling spectroscopic characterization and suggesting potential utility in catalysis and biological testing. Such behavior aligns with earlier reports on benzimidazole-based complexes [13, 14].

Antibacterial Activity. The free ligand demonstrated moderate inhibition of *S. aureus*, with a 13 mm suppression zone, but it failed to show any effect on *E. coli*. The Cu(II) complexes exhibited the highest antibacterial activity, as evidenced by inhibition zones of 24 mm for *S. aureus* and 15 mm for *E. coli*. The Zn(II) complexes displayed results that fell between the most and least effective

antibacterial activity. The results from Table 5 demonstrate that metal coordination makes bacteria more susceptible to treatment. The susceptibility differences between Gram+ and Gram- bacteria receive graphical representation in Fig. 5 [25–27].

The combination of Cu(II) with the compound resulted in maximum antibacterial effects which produced inhibition zones of 24 mm against *S. aureus* and 15 mm against *E. coli*.

The molecular properties of chelation lead to better lipophilicity and improved membrane penetration which enables the complex to enter bacterial cells and bind with biomolecules. The chelation process creates reactive oxygen species that damages bacterial membranes and produces oxidative stress according to research on benzimidazole–metal frameworks [28, 29].

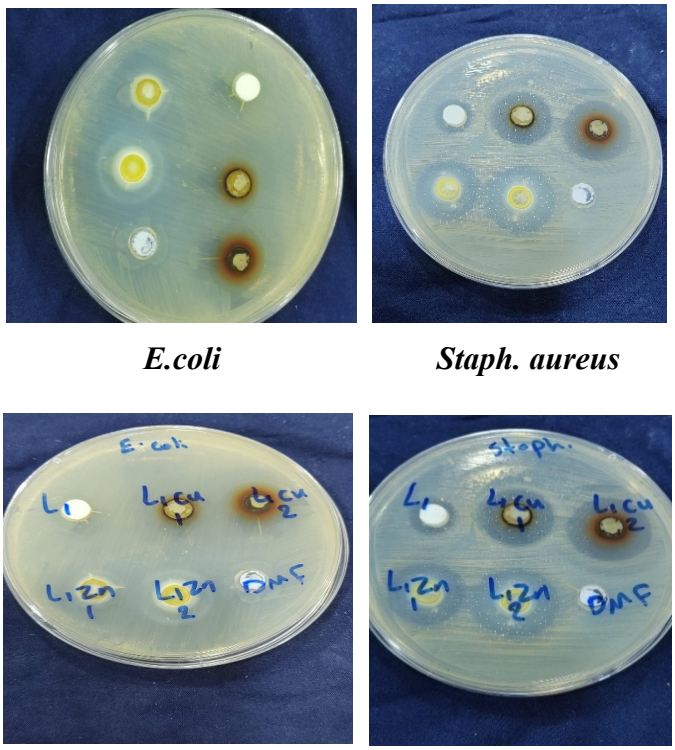

Fig. 5. Comparison of inhibition zones of ligand and complexes against *S. aureus* and *E. coli*.

Table 5. Antibacterial activity (inhibition zones, mm) of ligand and selected complexes

Number of Complexes	**Compound**	***Staphylococcus aurous* (mm)**	***Escherichia coli* (mm)**
1	$[Cu(L)_2]Cl_2$	20	11
2	$[Zn(L)_2]Cl_2$	19	8
3	$[Cu_2(L)_2(H_2O)_2]Cl_2$	24	15
4	$[Zn_2(L)_2(H_2O)_2]Cl_2$	22	7
L(Control)	$C_{16}H_{14}N_4S$	13	0
Solvent	DMF	0	0

The chelation process leads to increased metal ion polarity reduction and lipophilicity enhancement and better bacterial membrane permeability [26]. The Zn(II) complexes show better activity than the free ligand, yet their performance remains lower than that of Cu(II) complexes. The results support the chelation theory, which states that coordination enhances biological activity through better cellular uptake and biomolecule interaction [28, 30]. The observed stronger effect on Gram-positive bacteria matches previous research because their thick peptidoglycan layer provides less resistance to complex diffusion than the double membrane structure of Gram-negative bacteria [32–34].

Key Analytical Insights. Spectroscopic and magnetic data consistently indicate **tetrahedral geometry** around the metal centers.

- The ligand coordinates through **imidazole nitrogen** while the thioether sulfur remains non-coordinating.
- Antibacterial activity is **metal-dependent**, with Cu(II) > Zn(II) > free ligand.
- Gram-positive bacteria are more susceptible, reflecting differences in cell wall structure.

Conclusion

Metal complexes of bis((1H-benzo[d]imidazol-2-yl)methyl)sulfane with Mn(II), Co(II), Ni(II), Cu(II), and Zn(II) ions were synthesized and systematically investigated. Comprehensive characterization using elemental analysis, FTIR, UV–Vis and ^1H NMR spectroscopy, as well as molar conductivity and magnetic susceptibility measurements, indicated the formation of tetrahedral coordination geometries in both mononuclear and dinuclear species. Coordination occurs through the imidazole nitrogen atoms, whereas the thioether sulfur atom does not participate in metal binding.

All metal complexes exhibited enhanced antibacterial activity compared to the free ligand, with the Cu(II) complexes showing the highest efficacy against *Staphylococcus aureus* and *Escherichia coli*. These findings are consistent with chelation theory, as complex formation increases lipophilicity and reduces metal ion polarity, thereby facilitating penetration through bacterial cell membranes. In addition, Gram-positive bacteria were found to be more susceptible to the synthesized compounds, likely due to differences in cell envelope architecture.

Overall, this study highlights the potential of benzimidazole-based ligands as versatile scaffolds for the development of transition-metal complexes with promising antimicrobial properties. Furthermore, the structural and electronic flexibility of the benzimidazole framework suggests potential applications of the described complexes in catalytic oxidation, fluorescence sensing, and metal-based drug development.

References

1. Anand K., Wakode Sh. Development of Drugs on Benzimidazole Heterocycle: Recent Advancement and Insights. *International Journal of Chemistry Studies*, 2017, **Vol. 5(2)**, p. 350–362.
2. Chaviara A.T., Cox P.J., Repana K.H., Papi R.M., Papazisis K.T., Zambouli D., Kortsaris A.H., Kyriakidis D.A., Bolos C.A. Copper(II) Schiff Base Coordination Compounds of Dien with Heterocyclic Aldehydes and 2-Amino-5-Methyl-Thiazole: Synthesis, Characterization, Antiproliferative and Antibacterial Studies. Crystal Structure of Cu(dien)(OO)Cl_2. *Journal of Inorganic Biochemistry*, 2004, **Vol. 98**, p. 1271–1283. DOI: 10.1016/j.jinorgbio.2004.05.010
3. Aggoun D., Bouchareb S., Chafaa K., Garcia A.M. Synthesis, Crystal Structure, and Antimicrobial Activity of Transition Metal Complexes with Benzimidazole-Based Ligands. *Journal of Molecular Structure,* 2021, **Vol. 1239**, 130485. DOI: 10.1016/j.molstruc.2021.130485.
4. Suárez-Moreno Z.R., Cabrera M., Perez A.R., Fernandez J. Benzimidazole Derivatives as Multifunctional Ligands in Coordination Chemistry: A Review. *Coordination Chemistry Reviews,* 2022, **Vol. 460**, 214502. DOI: 10.1016/j.ccr.2022.214502.
5. Kizilcikli I., Ulkuseven B., Dasdemir Y., Akkurt B. Zn(II) and Pd(II) Complexes of Thiosemicarbazone-S-Alkyl Esters Derived from 2/3-Formylpyridine. *Synthesis and Reactivity in Inorganic, Metal-Organic, and Nano-Metal Chemistry*, 2004, **Vol. 34**, p. 653–665. DOI: 10.1081/SIM-120035948
6. Song W., Cheng J., Jiang D., Guo L., Cai M., Yang H., Lin Q. Synthesis, Interaction with DNA and Antiproliferative Activities of Two Novel Cu(II) Complexes with Schiff Base of Benzimidazole. *Spectrochimica Acta Part A: Molecular and Biomolecular Spectroscopy*, 2014, **Vol. 121**, p. 70–76. DOI: 10.1016/j.saa.2013.09.142

7. Sherif O.E., Abdel-Kader N.S. Spectroscopic and Biological Activities Studies of Bivalent Transition Metal Complexes of Schiff Bases Derived from Condensation of 1,4-Phenylenediamine and Benzopyrone Derivatives. *Spectrochimica Acta Part A: Molecular and Biomolecular Spectroscopy,* 2014, **Vol. 117**, p. 519–526. DOI: 10.1016/j.saa.2013.08.037
8. Kumar R., Mathur P. Aerobic Oxidation of 1,10-Phenanthroline to Phen-dione Catalyzed by Copper(II) Complexes of a Benzimidazolyl Schiff Base. *RSC Advances*, 2014, **Vol. 4**, p. 33190–33193. DOI:10.1039/c4ra03651d
9. Drozdzak R., Allaert B., Ledoux N., Dragutan I., Dragutan V., Verpoort F. Ruthenium Complexes Bearing Bidentate Schiff Base Ligands as Efficient Catalysts for Organic and Polymer Syntheses. *Coordination Chemistry Reviews,* 2005, **Vol. 249**, p. 3055–3074. DOI: 10.1016/j.ccr.2005.05.003
10. Zhang H., Xiang S., Xiao J. Heterogeneous Enantioselective Epoxidation Catalyzed by Mn(salen) Complexes Grafted onto Mesoporous Materials by Phenoxy Group. *Journal of Molecular Catalysis A: Chemical*, 2005, **Vol. 238**, p. 175–182.
11. Behpour M., Ghoreishi S.M., Soltani N., Niasari M.S. The Inhibitive Effect of Some Bis-N,S-Bidentate Schiff Bases on Corrosion Behaviour of 304 Stainless Steel in Hydrochloric Acid Solution. *Corrosion Science*, 2009, Vol. 51, p. 1073–1082. DOI: 10.1016/j.corsci.2009.02.011
12. Behpour M., Ghoreishi S.M., Mohammadi N., Niasari M.S. Investigation of the Inhibiting Effect of N-[(Z)-1-Phenylemethyleidene]-N-{2-[(2-{[(Z)-1-phenylmethylidene]amino}phenyl) disulfanyl]phenyl}amine and Its Derivatives on the Corrosion of Stainless Steel 304 in Acid Media. *Corrosion Science*, 2011, **Vol. 53**, p. 3380–3387. DOI: 10.1016/j.corsci.2011.06.017
13. El-Baradie K.Y., El-Wakiel N.A., El-Ghamry H.A. Synthesis, Characterization and Corrosion Inhibition in Acid Medium of l-Histidine Schiff Base Complexes. *Applied Organometallic Chemistry*, 2015, **Vol. 29(3)**, p. 117–125. DOI: 10.1002/aoc.3255
14. Kaim W., Schwederski B. *Bioinorganic Chemistry: Inorganic Elements in the Chemistry of Life*. 1996. New York. Wiley.
15. Murray R.K., Granner D.K., Mayes P.A., Rodwell V.W. *Harper's Biochemistry*. 1988. East Norwalk. CT: Appleton & Lange.
16. Kratz F., Nuber B., Weiss J., Keppler B.K. Synthesis and Characterization of Potential Antitumour and Antiviral Gallium(III) Complexes of N-Heterocycles. *Polyhedron*, 1992, **Vol. 11**, p. 487–498.
17. Mylonas S., Valavanidis A., Dimitropoulos K., Polissiou M., Tsiftsoglou A.S. Synthesis, Molecular Structure Determination, and Antitumor Activity of Platinum(II) and Palladium(II) Complexes of 2-Substituted Benzimidazole. *Journal of Inorganic Biochemistry*, 1988, **Vol. 34**, p. 265–275. DOI: 10.1016/0162-0134(88)83004-6
18. Kabanos T.A., Kersmidas A.D., Mentzafos D., Russo U., Terzis A., Tsangaris J.M. Synthesis, Structural and Physical Studies of Tin(IV) Complexes with 2-(2-Pyridyl)benzimidazole. *Journal of the Chemical Society, Dalton Transactions*, 1992, **Vol. 18**, p. 2729–2733. DOI: 10.1039/DT9920002729
19. Lalezari J.P., Aberg J.A., Wang L.H., Wire M.B., Miner R., Snowden W., Talarico C.L., Shaw S., Jacobson M.A., Drew W.L. Phase I Dose Escalation Trial Evaluating the Pharmacokinetics, Anti-Human Cytomegalovirus (HCMV) Activity, and Safety of 1263W94 in HIV-Infected Men with Asymptomatic HCMV Shedding. *Antimicrobial Agents and Chemotherapy*, 2002, **Vol. 46**, p. 2969–2976. DOI: 10.1128/AAC.46.9.2969-2976
20. Moreno M.J.S., Botello A.F., Coca R.B.G., Griesser R., Ochocki J., Kotynski A., Gutierrez J.N., Moreno V., Sigel H. Gallium Complexes of N-Heterocycles: Synthesis and Characterization. *Inorganic Chemistry*, 2004, **Vol. 43**, p. 1311–1322.
21. El-Sherif A.A. Mixed-Ligand Complexes of 2-(Aminomethyl) benzimidazole Palladium(II) with Various Biologically Relevant Ligands. *Journal of Solution Chemistry*, 2006, **Vol. 35**, p. 1287–1301.
22. Singh Ashok K., Kumar A., Katheria S., Jafri A., Arshad M. Design, Synthesis, Characterization, and Antiproliferative Activities of Ru(II) Complexes of Substituted Benzimidazoles. *Asian Journal of Chemistry*, 2019, **Vol. 31(10)**, p. 2311–2318.

23. Aghatabay N.M., Somer A., Karaböcek G., Ozkirimli B. Synthesis and Characterization of Metal Complexes with Benzimidazole Derivatives and Their Antimicrobial Activities. *Transition Metal Chemistry*, 2007, **Vol. 32**, p. 1111–1119. DOI:10.1007/s11243-007-0297-2
24. Aggoun D., Bouchareb S., Chafaa K., Garcia A.M. Synthesis, Crystal Structure, and Antimicrobial Activity of Transition Metal Complexes with Benzimidazole-Based Ligands. *Journal of Molecular Structure*, 2021, **Vol. 1239**, 130485. DOI: 10.1016/j.molstruc.2021.130485
25. Lopez-Sandoval H., Munoz G.D., Perez J., Ramirez A. Electronic Properties and Antimicrobial Studies of Benzimidazole Metal Complexes. *Polyhedron*, 2008, **Vol. 27**, p. 2942–2950. DOI: 10.1016/j.poly.2008.06.021
26. Mughal M.A., Rathore H.A., Bukhari S. Antimicrobial and DNA Binding Properties of Benzimidazole-Based Transition Metal Complexes. *Applied Organometallic Chemistry*, 2020, **Vol. 34(11)**, e5894. DOI:10.1002/aoc.5894
27. Suárez-Moreno Z.R., Cabrera M., Perez A.R., Fernandez J. Benzimidazole Derivatives as Multifunctional Ligands in Coordination Chemistry: A Review. *Coordination Chemistry Reviews,* 2022, **Vol. 460**, 214502. DOI: 10.1016/j.ccr.2022.214502.
28. Roaa R.A., Farah T.S. Synthesis and Characterization of Mn^{2+}, Co^{2+}, Ni^{2+}, Cu^{2+}, and Zn^{2+} Complexes with 4-(2-(Benzo-1,3-Dioxol-5-yl)-4,5-Diphenyl-2,5-Dihydro-1H-Imidazol-1-Yl)Aniline and Evaluation of Their Biological Activity. *Chemical Problems,* 2024, **Vol. 22(2)**, p. 197–210. DOI: 10.32737/2221-8688-2024-2-197-210
29. Pathan A.H., Shaikh R.A., Jadhav S.A. Synthesis and Characterization of Benzimidazole Metal Complexes and Their Antimicrobial Activities. *Spectrochimica Acta Part A: Molecular and Biomolecular Spectroscopy*, 2012, **Vol. 98**, p. 1–7. DOI:10.1016/j.saa.2012.07.029
30. Zalov A.Z., Hasanova N.S. Spectrophotometric study of ternar complexes of Cr (VI) and Co (II). *Chemical Problems*, 2020, **Vol. 2 (2),** p. 164-73. DOI: 10.32737/2221-8688-2020-2-164-173
31. Krátký M., Vinšová J. Antimicrobial Activity of Benzimidazole Derivatives and Their Metal Complexes. *Current Medicinal Chemistry,* 2012, **Vol. 19(33)**, p. 5419–5438. DOI: 10.2174/092986712803833268
32. Srivastava A.N., Gupta R. Antimicrobial and Antifungal Activity of Benzimidazole-Containing Metal Complexes. *European Journal of Medicinal Chemistry*, 2016, **Vol. 122**, p. 232–244. DOI: 10.1016/j.ejmech.2016.06.048
33. Ainscough E.W., Brodie A.M., Ranford J.D. Benzimidazole-Derived Copper Complexes: Spectroscopic Characterization and Antimicrobial Studies. *Inorganic Chemistry*, 1998, **Vol. 37(24)**, p. 6564–6572. DOI: 10.1021/ic981009a
34. Kratz F., Muller P. Coordination Chemistry of Benzimidazole Derivatives: Spectroscopic and Structural Insights. *Journal of Coordination Chemistry*, 1994, **Vol. 33(2),** p. 157–168. DOI: 10.1080/00958979408023943